JOC*Article*

Influence of Conformation on the EPR Spectrum of 5,5-Dimethyl-1-hydroperoxy-1-pyrrolidinyloxyl: A Spin Trapped Adduct of Superoxide

Gerald M. Rosen,*[,†,‡,§] Aleksandra Beselman,[†] Pei Tsai,[†] Sovitj Pou,[‡] Colin Mailer,[§,⊥] Kazuhiro Ichikawa,[§,⊥,∥] Bruce H. Robinson,[#] Robert Nielsen,[#] Howard J. Halpern,[§,⊥] and Alexander D. MacKerell, Jr.*[,†]

Department of Pharmaceutical Sciences, University of Maryland School of Pharmacy, Baltimore, Maryland 21201, Medical Biotechnology Center, University of Maryland Biotechnology Institute, Baltimore, Maryland 21201, Center for Low-Frequency EPR Imaging for In Vivo Physiology, The University of Chicago, Chicago, Illinois 60637, University of Maryland, Baltimore, Baltimore, Maryland 21201, Department of Radiation and Cellular Oncology, The University of Chicago, Chicago, Illinois 60637, and Department of Chemistry, University of Washington, Seattle, Washington 98195

grosen@umaryland.edu; amackere@rx.umaryland.edu

Received October 9, 2003

Spin trapping, a technique used to characterize short-lived free radicals, consists of using a nitrone or nitroso compound to "trap" an unstable free radical as a long-lived aminoxyl that can be characterized by EPR spectroscopy. The resultant aminoxyl exhibits hyperfine splitting constants that are dependent on the spin trap and the free radical. Such is the case with 2,2-dimethyl-5-hydroxy-1-pyrrolidinyloxyl (DMPO-OH) and 2,2-dimethyl-5-hydroperoxy-1-pyrrodinyloxyl (DMPO-OOH) whose hyperfine splitting constants, $A_N = A_H = 14.9$ G and $A_N = 14.3$ G, $A_H{}^{\beta} = 11.7$ G, and $A_H{}^{\gamma} = 1.25$ G, respectively, have been used to demonstrate the generation of $HO^{\bullet}$ and $O_2{}^{\bullet-}$. However, to date, the source of the apparent $A_H{}^{\gamma}$ hyperfine splitting in DMPO-OOH is not known. We consider three possible explanations to account for the unique EPR spectrum of DMPO-OOH. The first is that the γ-splitting arises from one of the hydrogen atoms at either carbon 3 or carbon 4 of DMPO-OOH. The second is that the γ-splitting originates from the hydrogen atom of DMPO-OOH. The third is that the conformational properties of DMPO-R change upon going from DMPO-OH to DMPO-OOH. Experimental and theoretical chemical approaches as well as EPR spectral modeling were used to investigate which of these hypotheses may explain the asymmetric EPR spectrum of DMPO-OOH. From these studies it is shown that the 12-line EPR spectrum of DMPO-OOH results not from any proximal hydrogen, but from additional conformers of DMPO-OOH. Thus, the 1.25 G hyperfine splitting, which has been assigned as a γ-splitting, is actually from two individual EPR spectra associated with different conformers of DMPO-OOH.

Introduction

In 1954, it was proposed that free radicals were the initiating event associated with oxygen poisoning and ionizing radiation.[1] It would take, however, another thirty years before cellular production of superoxide ($O_2{}^{\bullet-}$) and the accompanying cytotoxicity would be linked to the protective effects of the enzyme SOD (superoxide dismutase).[2] Evidence in support of this thesis comes, in part, from studies involving SOD-deficient bacteria.[3] Here, these mutants, when placed in an aerobic environment, were found to exhibit retarded growth, decreased viability, or enhanced frequency of spontaneous mutations. Drawing upon the sensitivity of microorganisms to $O_2{}^{\bullet-}$, humans have evolved unique cells, e.g., neutrophils that sequester $O_2{}^{\bullet-}$ in vacuoles to which microbes are phagocytosed therein. This pathway has been found to control microbial growth, the lack of which compromises the survival of the species.[4] However, more recent studies have suggested that $O_2{}^{\bullet-}$, in addition to its role in host

* Address correspondence to this author. Phone: 410-706-0514. Fax: 410-706-8184.
† University of Maryland School of Pharmacy.
‡ University of Maryland Biotechnology Institute.
§ Center for Low-Frequency EPR Imaging for In Vivo Physiology, The University of Chicago and University of Maryland.
⊥ Department of Radiation and Cellular Oncology, The University of Chicago.
∥ On leave from Kyushu University, Fukuoka, Japan.
University of Washington.

(1) Gerschman, R.; Gilbert, D. L.; Nye, S. W.; Dwyer, P.; Fenn, W. O. *Science* **1954**, *119*, 623−626.
(2) McCord, J. M.; Fridovich, I. *J. Biol. Chem.* **1969**, *244*, 6049−6055.
(3) (a) Carlioz, A.; Touati, D. *EMBO J.* **1986**, *5*, 623−630. (b) Natvig, D. O.; Imlay, K.; Touati, D.; Hallewell, R. A. *J. Biol. Chem.* **1987**, *262*, 14697-1701. (c) Storz, G.; Christman, M. F.; Sies, H.; Ames, B. N. *Proc. Natl. Acad. Sci. U.S.A.* **1987**, *84*, 8917−8921. (d) Nakayama, K. *J. Bacteriol.* **1992**, *174*, 4928−4934. (e) Nakayama, K. *J. Bacteriol.* **1994**, *176*, 1939−1943. (f) Longo, V. D.; Gralla, E. B.; Valetine, J. S. *J. Biol. Chem.* **1996**, *271*, 12275−12280.
(4) (a) Babior, B. M.; Kipnes, R. S.; Curnutte, J. T. *J. Clin. Invest.* **1973**, *52*, 741−744. (b) Malech, H. L.; Nauseef, W. M. *Semin. Hematol.* **1997**, *34*, 279−290.

10.1021/jo0354894 CCC: $27.50
Published on Web 01/17/2004

immune response, is involved in a number of signal transduction pathways.[5]

Future advances in understanding the importance of $O_2^{\bullet-}$ in a myriad of biological functions will depend, to a large extent, on identification of this free radical in real time. Of the available methods for the characterization of free radicals, spin trapping/EPR spectroscopy may be the most definitive of the analytical tools. Spin trapping, which was initially developed by Iwamura and Inamote[6] and later refined by Janzen and Blackburn,[7] consists of using a nitrone or nitroso compound to "trap" the initial unstable free radical as a long-lived aminoxyl that can be measured by EPR spectroscopy at ambient temperature.[8] For identification of the aminoxyl by EPR spectroscopy, the most important nearby source of magnetic field is derived from nuclei with magnetic moments in atoms in which the unpaired electron resides. The magnetic field of the nucleus will add to or subtract from the externally imposed magnetic field by a fixed amount, depending on its quantized orientation. This phenomenon results in splitting the absorption line. The magnitude of a splitting, therefore, depends on the size of the nuclear magnetic moment and the fraction of the electron spin density distribution at the particular nucleus. Multiple factors contribute to the spin density distribution, not all of which are fully understood.[9] The different splittings from nuclei yield a multiline EPR spectrum. The pattern of splittings often gives a unique signature, allowing the identification of a paramagnetic molecule.[10] In fact, this property is one of the great strengths of spin trapping/EPR spectroscopy. Even small differences between aminoxyls can frequently result in significant EPR spectral changes. Such is the case when $O_2^{\bullet-}$ and $HO^{\bullet}$ are spin trapped by DMPO (5,5-dimethyl-1-pyrroline *N*-oxide), leading to the hydroperoxyl and the hydroxyl spin trapped adducts, DMPO-OOH and DMPO-OH, respectively, which have distinctive EPR spectra.[8c] This ability to spectrally differentiate between DMPO-OOH and DMPO-OH has had a profound influence on our understanding of the role $O_2^{\bullet-}$ and $HO^{\bullet}$ play in many biological processes, including host immune response.[11] However, it remains unclear why the presence of an additional oxygen atom, e.g., DMPO-OOH versus DMPO-OH, should drastically alter the EPR spectrum of these aminoxyls.

SCHEME 1

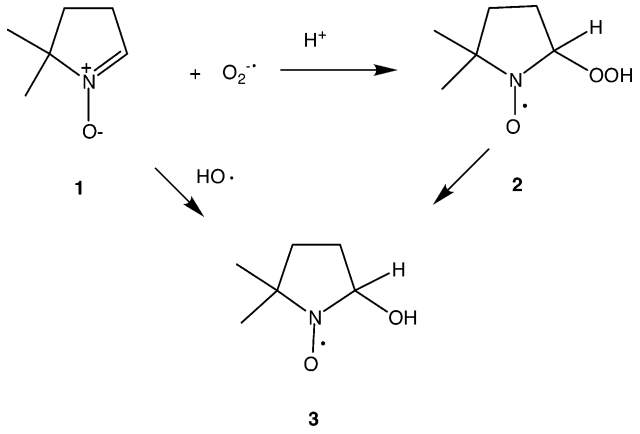

In this paper, we investigate how this hydroperoxyl group of DMPO-OOH influences the observed EPR spectrum via experimental, quantum mechanical,[12] and spectral modeling approaches.

Results and Discussion

Spin trapping/EPR spectroscopy offers the possibility of identifying short-lived free radicals based on the fact that the resultant spectral splitting constants of the aminoxyls are dependent on both the free radical and the spin trap.[9,10] As discussed above, nowhere is this uniqueness more evident than the contrasting EPR spectra of DMPO-OH and DMPO-OOH (Scheme 1, Figure 1, spectra A and B, respectively). An initial awareness of these differences came from experiments on the photolysis of H_2O_2.[13] At low concentrations of this peroxide in the presence of DMPO, an EPR spectrum corresponding to DMPO-OH was observed.[13] Interestingly, the structure of this aminoxyl is such that at 9.5 GHz, a four-line EPR spectrum was recorded with a relative peak ratio of 1:2:2:1 and hyperfine splitting constants of $A_N = A_H = 14.9$ G (Table 1).[13] At higher concentrations of H_2O_2, a second EPR spectrum was noted. This aminoxyl, with hyperfine splitting constants at 9.5 GHz of $A_N = 14.3$ G, $A_H^{\beta} = 11.7$ G, and $A_H^{\gamma} = 1.25$ G, was suggested to be DMPO-OOH.[13] These assignments were based exclusively on the established chemical reactions of $HO^{\bullet}$.

$$H_2O_2 + h\nu \rightarrow 2HO^{\bullet}$$

$$DMPO + HO^{\bullet} \rightarrow DMPO\text{-}OH$$

$$H_2O_2 + HO^{\bullet} \rightarrow HO_2^{\bullet} + H_2O$$

$$DMPO + HO_2^{\bullet} \rightarrow DMPO\text{-}OOH$$

Over the next several years, others would confirm these findings.[14]

(5) (a) Finkel, T. *J. Leukocyte Biol.* **1999**, *65*, 33−340. (b) Wolin, M. S. *Arterioscler. Thromb. Vasc. Biol.* **2000**, *20*, 1430−1442. (c) Droge, W. *Physiol. Rev.* **2002**, *82*, 47−95.

(6) Iwamura, M.; Inamoto, N. *Bull. Chem. Soc. Jpn.* **1967**, *40*, 703.

(7) (a) Janzen, E. G.; Blackburn, B. J. *J. Am. Chem. Soc.* **1968**, *90*, 5909−5910. (b) Janzen, E. G.; Blackburn, B. J. *J. Am. Chem. Soc.* **1969**, *91*, 4481−4490.

(8) (a) Janzen, E. G. *Acc. Chem. Res.* **1971**, *4*, 31−40. (b) Janzen, E. G. In *Free Radicals in Biology*; Pryor, W. A., Ed.; Academic Press: New York, 1980; Vol. 4, pp 116−154. (c) Finkelstein, E.; Rosen, G. M.; Rauckman, E. J. *Arch. Biochem. Biophys.* **1980**, *200*, 1−16.

(9) (a) Janzen, E. G.; Evans, C. A.; Liu, J. I.-P. *J. Magn. Reson.* **1973**, *9*, 513−516. (b) Janzen, E. G.; Liu, J. I.-P. *J. Magn. Reson.* **1973**, *9*, 510−512. (c) Engström, M.; Vaara, J.; Schimmellpfennig, B.; Ågren, H. *J. Phys. Chem. B.* **2002**, *106*, 12354−12360.

(10) (a) Buettner, G. R. *Free Radicals Biol. Med.* **1987**, *3*, 259−303. (b) Anson, S. W. L.; deHaas, A. H.; Buettner, G. R.; Chignell, C. F. *A Database for Spin-Trapping Implemented on the IBM PC*; Laboratory of Molecular Biophysics, National Institute of Environmental Health Sciences, 1989.

(11) (a) Britigan, B. E.; Rosen, G. M.; Chai, Y.; Cohen, M. S. *J. Biol. Chem.* **1986**, *261*, 4426−4431. (b) Pou, S.; Cohen, M. S.; Britigan, B. E.; Rosen, G. M. *J. Biol. Chem.* **1989**, *264*, 12299−12302. (c) Ramos, C. L.; Pou, S.; Britigan, B. E.; Cohen, M. S.; Rosen, G. M. *J. Biol. Chem.* **1992**, *267*, 8307−8312.

(12) Hehre, W. J.; Radom, L.; Schleyer, P. v. R.; Pople, J. A. *Ab Initio Molecular Orbital Theory*; John Wiley & Sons: New York, 1986.

(13) Harbour, J. R.; Chow, V.; Bolton, J. R. *Can. J. Chem.* **1974**, *52*, 3549−3553.

(14) (a) Finkelstein, E.; Rosen, G. M.; Rauckman, E. J. *Mol. Pharmacol.* **1979**, *16*, 676−685. (b) Kalyanaraman, B.; Perez-Reyes, E.; Mason, R. P. *Biochem. Biophys. Acta* **1980**, *630*, 119−130. (c) Mottley, C.; Connor, H. D.; Mason, R. P. *Biochem. Biophys. Res. Commun.* **1986**, *141*, 622−628.

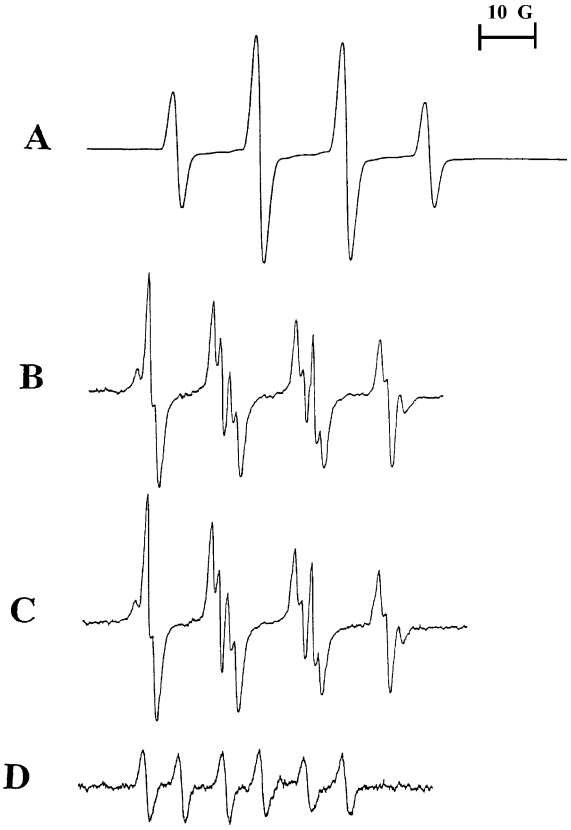

FIGURE 1. Representative EPR spectra of DMPO-OH, DMPO-OOH, DMPO-OOD, and M_4PO-OOH. (A) EPR spectrum of DMPO-OH, from the spin trapping of HO$^\bullet$ by DMPO, was obtained from the reduction of H_2O_2 (88 mM) by $FeSO_4$ (100 μM), receiver gain was 100. (B) EPR spectrum of DMPO-OOH, from the spin trapping of $O_2^{\bullet-}$ at an initial rate of 10 μM/min from the action of xanthine oxidase on hypoxanthine at pH 7.8, receiver gain was 8×10^3. (C) EPR spectrum of DMPO-OOD, from the spin trapping of $O_2^{\bullet-}$ at an initial rate of 10 μM/min from the action of xanthine oxidase on hypoxanthine. Reaction was conducted in D_2O in place of H_2O, receiver gain was 8×10^3. (D) EPR spectrum of M_4PO-OOH, from the spin trapping of $O_2^{\bullet-}$ at an initial rate of 10 μM/min from the action of xanthine oxidase on hypoxanthine at pH 7.8, receiver gain was 1.25×10^4. Hyperfine splitting constants of DMPO-OH, DMPO-OOH, and M_4PO-OOH are presented in Table 1.

TABLE 1. Reported Hyperfine Splitting Constants for the Studied Compounds

compd	A_N	A_H^β	A_H^γ	ref
DMPO-OH	14.9	14.9		13, 14
M_4PO-OH	15.3	16.9		15a
	15.3	16.5		15b
DMPO-OOH	14.3	11.7	1.25	13, 14
M_4PO-OOH	14.03	6.44		15a
	14.0	6.3		present study

What immediately struck us was the presence of an EPR spectrum of DMPO-OOH that contained an A_H^γ hyperfine splitting. Three possibilities were considered as explanations. The first was that the γ-splitting arises from one of the hydrogen atoms at either carbon 3 or carbon 4 of DMPO-OOH (Figure 2). Here, one of the hydrogen atoms may be sufficiently close to the aminoxyl to impose its nuclear spin on the unpaired electron. This possibility was supported by experiments with 3,3,5,5-tetramethyl-1-pyrroline *N*-oxide (M_4PO). In this case, the corresponding spin-trapped adducts of HO$^\bullet$ and $O_2^{\bullet-}$, M_4PO-OH, and M_4PO-OOH, respectively, gave the expected six-line spectra (Table 1 and Figure 1D).[15] In other experiments, the presence of A_H^γ hyperfine splitting was observed in DMPO-O-$(CH_2)_3CH_3$ but not in DMPO-$(CH_2)_3CH_3$ or DMPO-NH$(CH_2)_3CH_3$.[9a] In that study[9a] the increased A_H^γ hyperfine splitting was attributed to increased pucker of the five-membered ring due to increased electronegativity of the C2 substituents. Of note from that work[9a] was an A_H^γ hyperfine splitting of 1.63 G for the C3 or the C4 hydrogen in M_3PO-F with a fluorine as the C2 substituent. These findings suggest that the asymmetric EPR spectrum of DMPO-OOH may be associated with alterations in the puckering of the five-membered ring, increasing the spin density on the C3 or the C4 hydrogen, thereby leading to the A_H^γ hyperfine splitting.

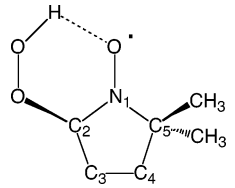

FIGURE 2. Diagram of DMPO-OOH showing the atom numbers and the possible hydrogen bond between the hydroperoxyl hydrogen atom and the aminoxyl oxygen.

The second possible explanation is that the γ-splitting arises from the hydrogen atom of the hydroperoxide of DMPO-OOH. By forming a hydrogen-bonded six-membered ring, this hydrogen atom might be sufficiently close to interact with the electron delocalized on the aminoxyl (Figure 2). A similar scenario has previously been investigated by using DMPO substituted with a series of alcohols.[16] These aminoxyls[16] can likewise form a six-membered ring, similar to that shown in Figure 2, with the hydroxyl group acting as a donor in a hydrogen bond with the aminoxyl oxygen. The EPR spectrum of DMPO-CH_2OH, for example, yielded six sharp lines, indicating that splitting by the hydrogen-bonded hydrogen atom was not occurring. However, DMPO analogues with more complex alcohols (e.g. DMPO-$CH(OH)CH_3$ or -$CH(OH)C_2H_5$) afforded asymmetric EPR spectra, analogous to that seen in DMPO-OOH. Use of perdeuterioethanol in that work showed that the asymmetry in the higher ordered alcohols was not due to the alcoholic hydrogen.[16] While these experiments indicated that hydrogen bonding (Figure 2) may not be responsible for the apparent γ-splitting in DMPO-OOH, we could not rule out this possibility, as the unique chemical nature of the hydroperoxide may allow for such a phenomenon to occur.

The third explanation is that changes in the conformational properties of DMPO-R occur upon going from DMPO-OH to DMPO-OOH. In this case, the 12-line EPR spectrum (Figure 1B) results, not from any proximal hydrogen, but from different conformers of DMPO-OOH. Thus, the 1.25-G hyperfine splitting (Table 1), which has

(15) (a) Rosen, G. M.; Turner, J. M., III *J. Med. Chem.* **1988**, *31*, 428−432. (b) Buettner, G. R.; Britigan, B. E. *Free Radicals Biol. Med.* **1990**, *8*, 57−60.

(16) Kotake, Y.; Kuwata, K.; Janzen, E. G. *J. Phys. Chem.* **1979**, *83*, 3024−3029.

been assigned as a γ-splitting, is actually due to superimposed EPR spectra associated with individual conformers.

This paper describes investigations to determine which of the three possible explanations is plausible. We approached this problem from the standpoint of experimental findings and theoretical considerations. Then, based on these data, EPR spectra were modeled with use of a global analysis method.

For the initial hypothesis, studies with $HO^{\bullet}$ and $O_2^{\bullet-}$ spin trapped adducts of DMPO and M_4PO were performed via quantum mechanical (QM) calculations to determine if alterations in ring puckering would allow either the C3 or the C4 hydrogen atoms to generate the γ-splitting. Further, experiments supported by QM results were conducted to address the possible role of a hydrogen bond between the aminoxyl oxygen and the hydrogen atom from the hydroperoxide as suggested by hypothesis two. In the case of hypothesis three, QM calculations were performed to determine if DMPO-OOH accesses additional conformations that may explain the asymmetric EPR spectrum. Results from the QM computations were then verified via simulation of the experimental EPR spectrum of DMPO-OOH.

Deemed essential to validate the present conclusion was that data be consistent with the EPR spectrum of DMPO-OH, DMPO-OOH, M_4PO-OH, and M_4PO-OOH. Presented in Table 1 are the hyperfine splitting constants for these four aminoxyls. Of note are the identical A_N and A_H^{β} hyperfine splitting of DMPO-OH, leading to a four-line EPR spectrum and the presence of apparent A_H^{γ} splitting in DMPO-OOH, resulting in the 12-line, asymmetric EPR spectrum.

C3 or C4 γ-Splitting. We consider the first hypothesis that the 12-line EPR spectrum of DMPO-OOH is due to a γ-splitting of a hydrogen atom at either the C3 or the C4 position of DMPO-OOH. As stated above this theory was supported by the EPR spectrum of M_4PO-OOH, which contained the expected six lines.[15] While these data support the absence of γ-splitting at C3, these findings do not explain why there is no γ-splitting at C4. Consistent with the suggestion by Janzen et al.,[9a] this finding indicated that changes in ring puckering occurred, leading to the A_H^{γ} hyperfine splitting. To investigate the possibility that such changes were taking place, QM calculations were performed on DMPO-OH, DMPO-OOH, M_4PO-OH, and M_4PO-OOH. Presented in Table 2 are the N1−C2−C3−C4, C2−C3−C4−C5, and C3−C2−N1−O dihedral angles for the two ring puckers of each compound. The two ring puckers are referred to as pucker 1 and pucker 2 corresponding to C2−C3−C4−C5 dihedral angles (Figure 2) of ca. 30° and −30°, respectively. Included in Table 2 are the dihedrals, defining the orientation of the hydroxyl and hydroperoxyl groups on DMPO and M_4PO. Comparison of the ring dihedrals shows the majority of values to be similar for DMPO-OH and DMPO-OOH, with the greatest difference being 4° for N−C−C−C. The two M_4PO analogues also yield similar ring conformations. Comparison of the DMPO and M_4PO ring conformations, however, indicates that the presence of the dimethyl group, rather than the hydroperoxyl group, has a larger impact on the ring structure. For example, the N−C−C−C dihedral in pucker 2 changed by 10° upon going from DMPO-OH to M_4PO-OH and 14° between DMPO-OOH and M_4PO-OOH.

TABLE 2. Dihedral Angles Defining the Conformation of the Ring Pucker and the Hydroxyl or the Hydroperoxyl Substituent for the UHF/6-31++G(d,p) Minimum Energy Structures[a]

	N-C-C-C	C-C-C-C	O-N-C-C	N-C-O-H
DMPO-OH				
pucker 1	329	35	186	303
pucker 2	24	326	166	309
M_4PO-OH				
pucker 1	327	28	188	300
pucker 2	34	331	170	312

	N-C-C-C	C-C-C-C	O-N-C-C	N-C-O-O	C-O-O-H
DMPO-OOH					
pucker 1	330	34	185	270	84
pucker 2	20	327	165	270	83
M_4PO-OOH					
pucker 1	329	27	188	281	71
pucker 2	34	330	166	281	73

[a] Dihedral angles in degrees. N−C−C−C is N1−C2−C3−C4, C−C−C−C is C2−C3−C4−C5, and O−N−C−C is O−N1−C2−C3. Geometries correspond to the minimum energy structures presented in Figure 3.

TABLE 3. Distances in Å between the Nitrogen and Position 3 or 4 Hydrogen Atoms for the UHF/6-31++G(d,p) Minimum Energy Structures[a]

	H3′	H3″	H4′	H4″
DMPO-OH				
pucker 1	3.24	2.78	2.85	3.24
pucker 2	2.85	3.24	3.25	2.79
M_4PO-OH				
pucker 1			2.98	3.18
pucker 2			3.19	2.97
DMPO-OOH				
pucker 1	3.24	2.77	2.86	3.24
pucker 2	2.88	3.23	3.25	2.77
M_4PO-OOH				
pucker 1			2.98	3.19
pucker 2			3.19	2.96

[a] Pucker 1 and pucker 2 correspond to the minimum energy structures associated with C2−C3−C4−C5 angles of ca. 30° and −30°, respectively. H3′ and H4′ are located on the same face of the ring as the hydroxyl or peroxide moieties and H3″ and H4″ are on the opposite face.

To understand how the changes in the ring structure impact the distance of the hydrogen atoms at C3 and C4 to the aminoxyl N, the H to N distances for the structures in Table 2 were determined and are presented in Table 3.

Consistent with the ring dihedrals, the distances between the hydrogen atoms and the ring nitrogen are within 0.02 Å for DMPO-OH and DMPO-OOH and within 0.01 Å for M_4PO-OH and M_4PO-OOH. Finally, Mulliken overlap populations were analyzed to determine if a significant increase in orbital overlap between the aminoxyl N and the γ-hydrogen atoms occurred in DMPO-OOH. While the use of Mulliken overlap populations is limited, as previously discussed,[17] the relative values may be considered reliable enough to indicate if significant overlap were occurring in one compound as compared to

(17) Kong, S.; Evanseck, J. D. *J. Am. Chem. Soc.* **2000**, *122*, 10418−10427.

TABLE 4. Mulliken Overlap between the Nitrogen and the Position 3 or 4 Hydrogens for the UHF/6-31++G(d,p) Minimum Energy Structures[a]

	H3′	H3″	H4′	H4″
DMPO-OH				
pucker 1	0.003645	0.000777	0.001256	0.003092
pucker 2	−0.001266	0.003172	0.003690	−0.000526
M_4PO-OH				
pucker 1			0.017458	0.006362
pucker 2			0.014952	−0.016621
DMPO-OOH				
pucker 1	0.008923	0.014920	0.014653	0.015183
pucker 2	−0.000573	0.003221	0.003525	−0.000705
M_4PO-OOH				
pucker 1			0.013213	0.008507
pucker 2			0.002342	−0.003402

[a] Pucker 1 and pucker 2 correspond to the minimum energy structures associated with C2−C3−C4−C5 angles of ca. 30° and −30°, respectively. H3′ and H4′ are located on the same face of the ring as the hydroxyl or peroxide moieties and H3″ and H4″ are on the opposite face.

TABLE 5. Relative Energies of DMPO-OH, M_4PO-OH, DMPO-OOH, and M_4PO-OOH as a Function of Ring Conformation[a]

structure	pucker 1	transition state	pucker 2
potential energies, UHF/6-31G*			
DMPO-OH	0.00	1.77	0.53
M_4PO-OH	0.00	1.77	0.88
DMPO-OOH	0.12	1.81	0.00
M_4PO-OOH	0.00	1.59	0.37
potential energies, UHF/6-31++G**			
DMPO-OH	0.00	2.02	0.53
M_4PO-OH	0.00	1.84	0.71
DMPO-OOH	0.14	1.90	0.00
M_4PO-OOH	0.00	1.62	0.20

[a] Energies in kcal/mol. Pucker 1 and pucker 2 correspond to C2−C3−C4−C5 angles of ca. 30° and −30°, respectively. Structures correspond to the global minima presented in Figure 3 following full optimization.

others that could result in γ-splitting. Data, presented in Table 4, show the largest overlaps to occur with M_4PO-OH, where no γ-splitting occurs, followed by DMPO-OOH, indicating that γ-splitting is not responsible for the asymmetry of DMPO-OOH.

Moreover, comparison of the values for DMPO-OH and M_4PO-OH demonstrates that the presence of additional methyl groups leads to significant changes in overlap populations. Thus, the lack of significant changes in the ring pucker upon going from the hydroxyl to the hydroperoxyl analogues combined with the lower Mulliken overlap populations in DMPO-OOH versus M_4PO-OOH indicate that γ-splitting is not responsible for the asymmetric spectrum of DMPO-OOH. Interestingly, the presence of dimethyl groups at C3 is predicted by the QM computations to have a greater impact on ring pucker than the presence of the hydroperoxyl group. This finding is consistent with differences in the magnitude of A_N and A_H^{β} hyperfine splitting constants between aminoxyls derived from DMPO and M_4PO (Table 1).

Hyperfine Splitting via Hydrogen Bonding between the Aminoxyl and the Hydroperoxide. Previous experiments with either DMPO-CH(OH)CH_3 or DMPO-CH(OH)C_2H_5 indicated that an interaction of the hydrogen in a six-membered ring formed by a hydrogen bond with the oxygen atom (Figure 2) would not produce the obtained asymmetric EPR spectrum of DMPO-OOH,[9a] as discussed above. The structure of DMPO-OOH, however, could alter the nature of the interaction leading to the apparent γ-splitting. If this possibility were true, then conducting the spin-trapping experiment in D_2O would result in a different EPR spectrum. While the strength of the hydrogen bond may be stronger by substituting deuterium at this position,[18] the γ-splitting of 1.25 G should collapse to 0.18 G and the number of spectral lines should increase to 18.[19] When a series of experiments were conducted to test this hypothesis, there was no difference in the EPR spectrum between DMPO-OOH and DMPO-OOD (Figure 1, spectra B and C). These data demonstrated that the hyperfine splitting of 1.25 G was not the result of a hydrogen atom from the hydroperoxide interacting with the NO of the aminoxyl.

Consistent with these results is the calculated structures of DMPO-OOH and M_4PO-OOH. In both compounds the hydrogen atom on the hydroperoxide points toward the aminoxyl oxygen, due to a favorable hydrogen bond interaction. However, the interaction distances are shorter in M_4PO-OOH, with H-O distances of 2.28 and 2.12 Å for pucker 1 and pucker 2, respectively, versus distances of 2.59 and 2.42 Å for DMPO-OOH. If the hydroperoxide hydrogen were responsible for the splitting in DMPO-OOH, shorter distances would be expected in DMPO-OOH as compared to M_4PO-OOH.

Conformational Characteristics. The final hypothesis for the 12-line EPR spectrum of DMPO-OOH is the presence of unique conformers of DMPO-OOH that could lead to overlapping EPR spectra. To investigate this possibility, QM computations were undertaken on DMPO-OH, DMPO-OOH, M_4PO-OH, and M_4PO-OOH to determine conformations accessible to the different compounds. The conformational properties of these aminoxyls may be separated into those associated with (a) puckering of the pyrrolidinoxyl ring or (b) rotation of the hydroxyl or hydroperoxyl groups.

Investigation of the influence of the pyrrolidinoxyl puckering was undertaken by optimizing the structures for the two ring conformations (e.g., pucker 1 and pucker 2, where the C2−C3−C4−C5 dihedral is ca. 30° and −30°, respectively) along with the planar conformation (e.g., C2−C3−C4−C5 = 0°), which represent the putative transition state between the two ring puckers. Presented in Table 5 are the relative energies of the two ring puckers for each species studied, along with the relative energy of the barrier to rotation. Concerning the relative energies of the two puckered geometries, in all cases the higher energy pucker is 0.9 kcal/mol or less, indicating that both ring puckers can be sampled in all cases. Moreover, for all four compounds, the putative barrier heights are similar, indicating that dynamic properties of the ring are not significantly influenced by the substitution at C2. These results indicate that significant differences in the population of the two ring puckers are not contributing to the additional splitting seen in the asymmetric EPR spectrum of DMPO-OOH.

(18) (a) Dalhgren, G., Jr.; Long, F. A. *J. Am. Chem. Soc.* **1960**, *82*, 1303−1308. (b) Creswell, C. J.; Allred, A. L. *J. Am. Chem. Soc.* **1962**, *84*, 3966−3967.

(19) Halpern, H. J.; Pou, S.; Peric, M.; Yu, C.; Barth, E.; Rosen, G. M. *J. Am. Chem. Soc.* **1993**, *115*, 218−223.

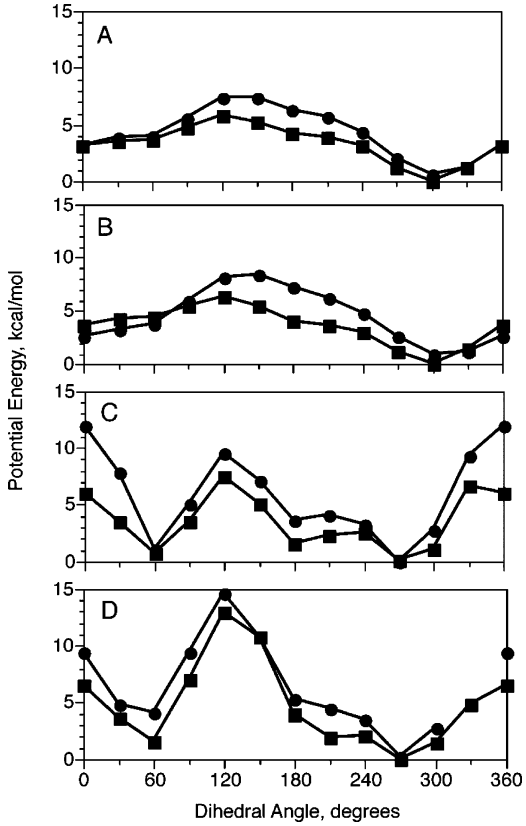

FIGURE 3. Potential energy surfaces for the C2−O dihedral for (A) DMPO-OH, (B) M_4PO-OH, (C) DMPO-OOH, and (D) M_4PO-OOH. Surfaces are presented with the rings in both the pucker 1 (squares, C2−C3−C4−C5 = ca. 30°) and pucker 2 (circles, C2−C3−C4−C5 = ca. −30°) orientations. Note that the ring pucker was allowed to relax during the optimizations. The omitted point at 330° in the M_4PO-OOH (D) surface was due to the ring pucker switching from the −30° region to the 30° region.

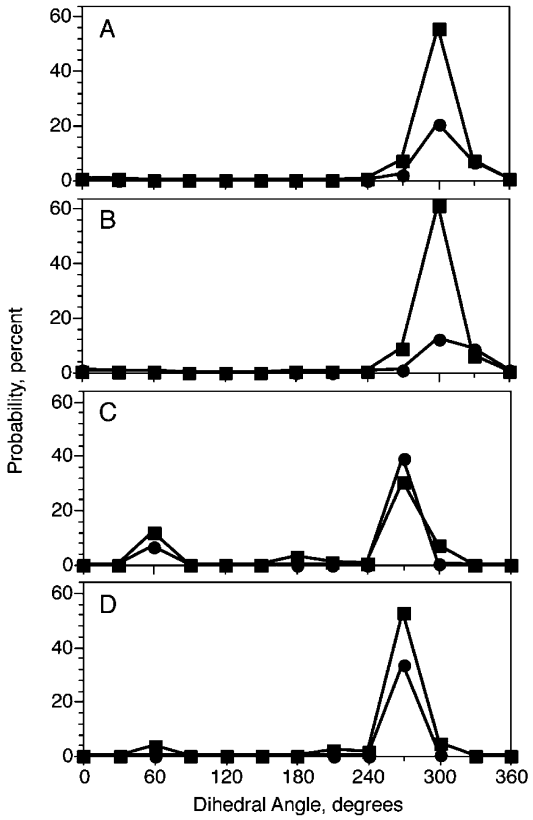

FIGURE 4. Probability distributions for the C2−O dihedral for (A) DMPO-OH, (B) M_4PO-OH, (C) DMPO-OOH, and (D) M_4PO-OOH. Distributions are presented with the rings in both the pucker 1 (squares, C2−C3−C4−C5 = ca. 30°) and pucker 2 (circles, C2−C3−C4−C5 = ca. −30°) orientations. Note that the ring pucker was allowed to relax during the optimizations.

Computations were next performed to determine if possible contributions from rotation of the hydroxyl or the hydroperoxyl group yielded alternate, stable conformations leading to the asymmetric spectrum. Potential energy surfaces were determined for the N1−C2−O−H and N1−C2−O−O dihedrals for both ring puckers in all four compounds. These surfaces are presented in Figure 3. For DMPO-OH and M_4PO-OH (Figure 3A,B), there is a single minimum for both puckers at 300° with the DMPO-OH and M_4PO-OH surfaces being similar. The minimum at 300° corresponds to the orientation of the hydroxyl group in which the hydrogen atom can interact most favorably with the oxygen of the aminoxyl. The surfaces for the hydroperoxyls are more complicated as compared to the hydroxylated aminoxyls. For both DMPO-OOH (Figure 3C) and M_4PO-OOH (Figure 3D) there are minima at 60° and 270°. In both cases, the 270° minimum is of lower energy for both puckers; however, in DMPO-OOH the relative energies of the 60° minimum are only 0.7 and 1.1 kcal/mol above the global minimum. In M_4PO-OOH the minimum at 60° are 1.6 and 4.0 kcal/mol above the global minimum. Also of note is the higher energy barrier in the M_4PO-OOH at 120° as compared to DMPO-OOH. This higher energy barrier, along with the higher relative energy of the minimum at 60° in M_4PO-OOH, is due to steric overlap of the hydroperoxyl and the dimethyl groups at C3. Thus, substitution at C2 by the hydroperoxyl group leads to the presence of two minima, with the relative values of the minimum influenced by the presence of the dimethyl substitution at C3.

To better visualize the impact of the dimethyl substitution at C3 on the conformational properties, the energy surfaces in Figure 3 were converted into probability distributions based on a Boltzmann distribution.[20] This treatment allows for quantization of the conformations that will be sampled by the different compounds. Presented in Figure 4 are the probability distributions, which have been normalized to 100% with respect to the global minimum of both ring puckers. Consistent with the energy surfaces, DMPO-OH and M_4PO-OH populate only the region in the vicinity of 270°. A similar pattern is calculated for M_4PO-OOH (Figure 4D) where the region in the vicinity of 270° is the most populated, although the region around 60° for the 30° pucker is indicated to be negligibly populated (ca. 5%). In contrast, DMPO-OOH significantly populates both the 60° region (ca. 20%) and the 270° region. Thus, the QM computations indicate that DMPO-OOH assumes conformations based on two distinct orientations of the hydroperoxyl group, with the second conformation not being as accessible in M_4PO-

(20) (a) McQuarrie, D. A. *Statistical Mechanics*; Harper & Row: New York, 1976. (b) Yang, B.; Wright, J.; Eldefrawi, M. E.; Pou, S.; MacKerell, A. D., Jr. *J. Am. Chem. Soc.* **1994**, *116*, 8722−8732.

OOH due to steric overlap of the hydroperoxide group and the dimethyl substitutent at C3. On the basis of these results it is suggested that the 6-line EPR spectrum of M_4PO-OOH is due to a single dominant conformer, while in DMPO-OOH, two conformations are accessible, leading to the asymmetric 12-line EPR spectrum shown in Figure 1B.

Line Width Analysis. To validate the hypothesis that the asymmetric EPR spectrum of DMPO-OOH is due to two accessible conformations, EPR spectra were modeled with use of a global analysis method. To this end, we modified the algorithms of Robinson et al. [21] developed to fit single nitroxide spectra such that EPR spectra with different populations of contributing aminoxyls could be simulated.[22] An important feature of the program is that it allows the linkage of parameters. For example, the widths or intensities of spectral lines of a set of EPR spectra can be forced to be equal, even though the actual values of the line width or intensity are not known a priori.

The first model examined was that where the EPR spectrum is due to γ-splitting in DMPO-OOH with hyperfine splittings of 13.8 G for ^{14}N, 10.99 G for the ^{1}H at C2, and 1.19 G from a single γ-^{1}H splitting at either C3 or C4 (i.e., the current model based on γ-splitting). The EPR spectrum shown in Figure 5 is made up of DMPO-OOH and its decomposition product, DMPO-OH. At the time the EPR spectrum was recorded (~3 min after the reaction began) the ratio of these aminoxyls was 9:1. Figure 5A shows the experimental EPR spectrum and the best-fit simulation, respectively. While the overall fit is reasonable, especially with respect to the location of the peaks, the level of agreement for the intensities is not ideal.

The second model tested included contributions from two DMPO-OOH conformations to the EPR spectrum, as motivated by the QM results. When considering this model an immediate question is whether the two conformers of DMPO-OOH have different *g*-values or whether they have different hyperfine splittings? To exclude a possible contribution from different *g*-values, which are sensitive to frequency, spin-trapping experiments were carried out at the Medical College of Wisconsin National EPR Center on DMPO-OOH at S-band (3.5 GHz). Results showed that a *g*-value difference could not be the reason, as the S-band EPR spectrum (not shown) was identical with that acquired at X-band (9.5 GHz). Hence, the DMPO-OOH spectrum must be due to two conformers having different hyperfine tensors. Accordingly, EPR spectra were modeled with identical ^{14}N tensor values but different ^{1}H hyperfine splittings for the two conformers. The EPR spectrum depicted in Figure 5B shows that all data are well fitted by the model with both conformers having the same ^{14}N tensor value of 13.77 G with one conformer having a ^{1}H hyperfine splitting of 12.19 G and the other a ^{1}H hyperfine splitting of 9.78 G. As is evident both peak locations and magnitudes are well fitted. This quality of fit supports the model that the complex spectra are due to two individual conformations of DMPO-OOH yielding the observed EPR spectra.

Finally, the relative proportion of these two conformations is open to interpretation. This question was addressed via analyses into mechanisms of line width broadening for aminoxyl esters.[22] We modeled the EPR spectra of the conformers including the (unresolved) hyperfine splittings of the four γ-^{1}H's and three methyl ^{1}H's. It was observed that the best fit came from the unequal-population case with the populations of the DMPO-OOH conformers being 54% to 46% as shown in Figure 5B.

Presented in Figure 6 are the two stable DMPO-OOH structures with the ring conformation in pucker 2. Comparison of the structures shows the different spatial relationship of the OH atoms of the hydroperoxyl with respect to the N−O group. It is suggested that the differential orientation of the dipole associated with the OH atoms leads to an altered magnetic environment of the radical, yielding different ^{1}H hyperfine splittings for the two conformers. This different splitting combined with the presence of the two conformers leads to the asymmetric EPR spectra of DMPO-OOH.

Conclusion

Presented is a combination of results from experimental, theoretical, and EPR spectral modeling studies on DMPO-OH, M_4PO-OH, DMPO-OOH, and M_4PO-OOH. These findings, in combination with previously available data, were used to identify the origin of the 12-line EPR spectrum of DMPO-OOH, whose unique characteristics have been exploited to detect $O_2^{\bullet-}$ in a wide variety of biological and chemical systems. On the basis of this information, the asymmetric EPR spectrum of DMPO-OOH is concluded to be due to two conformations of DMPO-OOH, yielding two overlapping EPR spectra. While we are not the first to propose this hypothesis,[23] we are the first to use theoretical and spectral modeling studies of EPR spectra to support experimental data. In the earlier publication,[23] it was suggested that the EPR spectrum of DMPO-OOH is derived from two conformers of equal population with $A_H^\gamma = 1.1$ G for one and $A_H^\gamma = 1.4$ G for the other. This is contrary to our data.

Importantly, possible contributions associated with either γ-splitting of the unpaired electron by the hydroperoxyl hydrogen atom or γ-splitting by C3 and C4 hydrogen atoms have been eliminated based on EPR spectral data for M_4PO-OH and M_4PO-OOH combined with computed geometries and experiments with D_2O.

The present hypothesis concerning the 12-line spectra of DMPO-OOH has the advantage that it also explains the EPR spectra of DMPO-OH, M_4PO-OH, and M_4PO-OOH (Table 1). Experimental EPR spectra of DMPO-OH and M_4PO-OH are similar, consistent with conformational properties of the hydroxyl group (Figure 3, spectra A and B). Subtle changes in the conformation of the five-membered ring (Table 2) may contribute to small changes in the A_N and A_H^β hyperfine splitting constants. For

(21) (a) Robinson, B. H.; Mailer, C.; Reese, A. W. *J. Magn. Reson.* **1999**, *138*, 199−200. (b) Robinson, B. H.; Mailer, C.; Reese, A. W. *J. Magn. Reson.* **1999**, *138*, 210−219. (c) Mailer, C.; Robinson, B. H.; Williams, B. B.; Halpern, H. J. *Magn. Reson. Med.* **2003**, *49*, 1175−1180.

(22) Tsai, P.; Ichikawa, K.; Mailer, C.; Pou, S.; Halpern, H. J.; Robinson, B. H.; Nielsen, R.; Rosen, G. M. *J. Org. Chem.* **2003**, 60, 7811−7817.

(23) Frejaville, C.; Karoui, H.; Tuccio, B.; Le Moigne, F.; Culcasi, M.; Pietri, S.; Lauricella, R.; Tordo, P. *J. Med. Chem.* **1995**, *38*, 258−265.

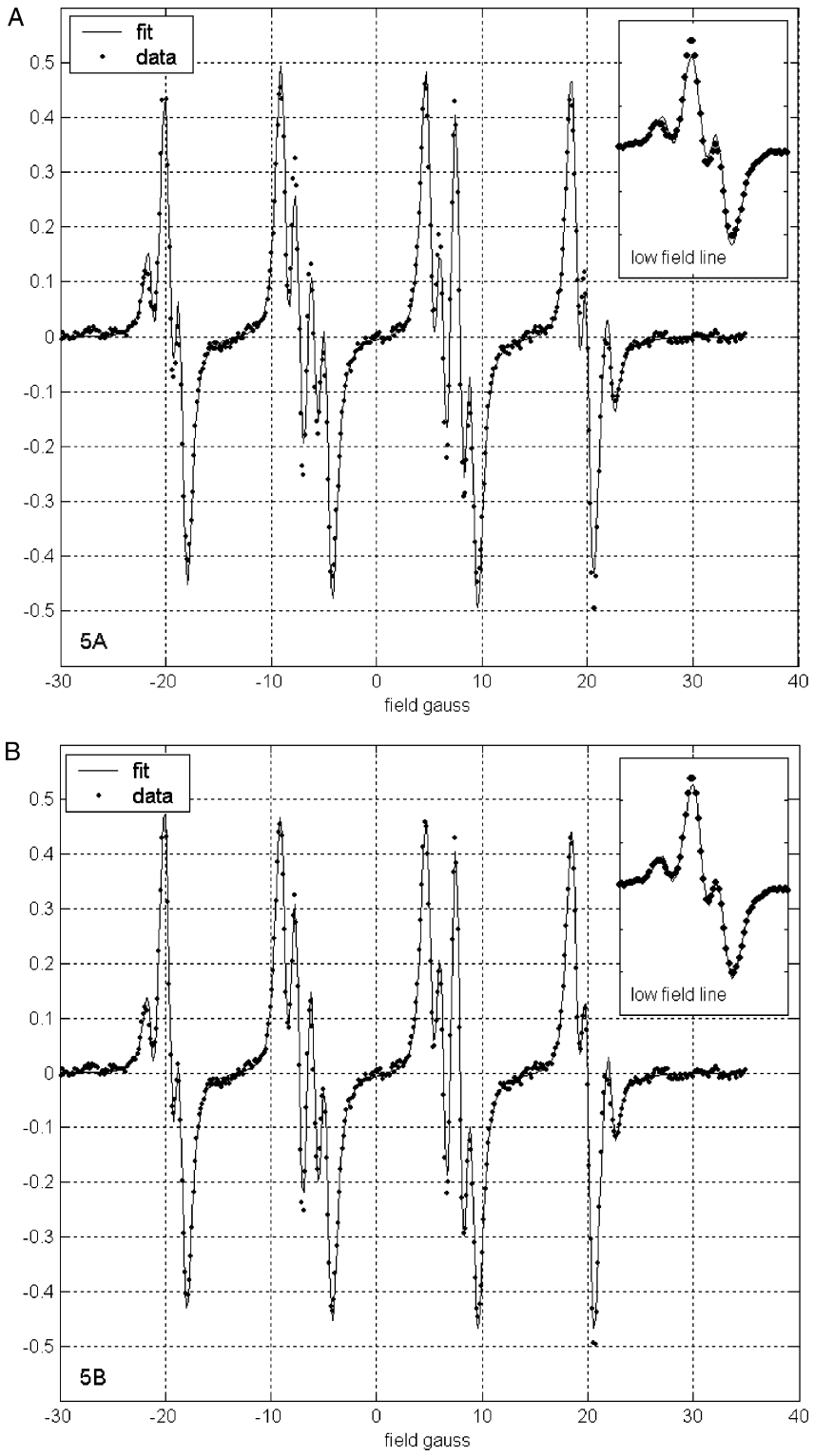

FIGURE 5. (A) EPR experimental spectrum (dots) at X-band and the best-fit simulation (line), respectively, for a single γ-^{1}H model of the DMPO-OOH conformers and the decomposition product DMPO-OH. The inset at the top right is an expanded plot of the low-field line. Fitting parameters for the DMPO-OOH are the following: hyperfine splittings of 13.8 G for ^{14}N, 10.99 G for the ^{1}H at the 2-position, and 1.19 G from a single γ-^{1}H splitting at either C3 or C4; the line width was 0.512 G. Fitting parameters for the DMPO-OH are the following: hyperfine splittings of 14.7 for ^{14}N, 14.2 G for the ^{1}H at C2, and a line width of 0.68 G. The ratio of DMPO-OOH to DMPO-OH is 9:1. (B) EPR experimental spectrum (dots) at X-band and the best-fit simulation (line), respectively, for the model with both DMPO-OOH conformers and the decomposition product, DMPO-OH. The conformers have the same ^{14}N tensor value of 13.77 G but one conformer has a ^{1}H hyperfine splitting of 12.19 G and the other a ^{1}H hyperfine splitting of 9.78 G. The inset at the top right is an expanded plot of the low-field line. Fitting parameters for the DMPO-OH are the following: hyperfine splittings of 14.7 for ^{14}N, 14.2 G for the ^{1}H at C2, and a line width of 0.68 G. The ratio of DMPO-OOH to DMPO-OH is 9:1.

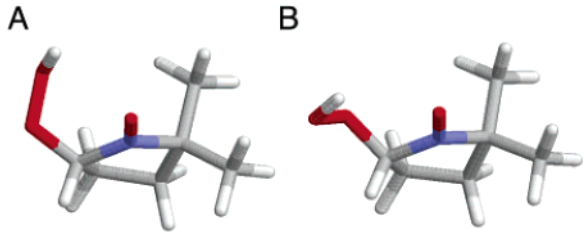

FIGURE 6. Structures of DMP-OOH with the N1−C2−O−O dihedral at approximately (A) 60° and (B) 270° for ring pucker 2. Structures are fully optimized at the UHF/6-31++G(d,p) level of theory.

DMPO-OOH and M_4PO-OOH, the presence of the hydroperoxyl group alters the EPR spectrum of each aminoxyl by significantly changing the A_H^{β} hyperfine splitting constants, apparently due to the more electronegative character of the hydroperoxyl as compared to the hydroxyl group. In M_4PO-OOH, the six-line spectrum is consistent with the hydroperoxyl group only significantly occupying one conformation (Figures 3D and 4D). In contrast, the hydroperoxyl in DMPO-OOH significantly populates two conformations (Figures 3C and 4C). The two conformations are suggested to each contribute an individual six-line EPR spectrum, combining to yield the asymmetric experimental EPR spectrum shown in Figure 1B. The interpretation is consistent with the asymmetric EPR spectra of DMPO substituted with complex alcohols (i.e. DMPO-$CHOHCH_3$ or -$CHOHC_2H_5$),[9a] where it is suggested that the complexity of the substituent (versus, for example, -CH_2OH) leads to multiple stable conformations, yielding overlapping EPR spectra as observed with DMPO-OOH. Of note is that the two different conformers of DMPO-OOH have nearly identical hyperfine splitting constants for ^{14}N (Figure 5). This suggests that the orientation of the hydroperoxyl group does not significantly influence the ^{14}N hyperfine splitting, just the ^1H hyperfine splitting. Rather, based on comparison of the splitting constants for DMPO-OOH and M_4PO-OOH, as well as for DMPO-OH and M_4PO-OH (Table 1), changes in ring pucker due to the presence of the dimethyl group on C3 are suggested to lead to the changes in the ^{14}N hyperfine splitting.

While the experiments described herein were conducted under specific conditions, it is worth discussing, although briefly, the impact the environment has on hyperfine splittings. In homogeneous solvents, the isotropic ^{14}N hyperfine coupling constant (A_{iso}) can be written as a sum of two terms $A_{iso} = A_{iso}^{e} + A_{iso}^{h}$, where A_{iso}^{e} is the electrostatic interaction term and A_{iso}^{h} is the hydrogen bonding term. Onsager theory shows a linear relationship between A_{iso} and $\epsilon - 1/\epsilon + 1$ for aminoxyls in aprotic solvents ($A_{iso}^{h} = 0$) with dielectric constant ϵ. That is, A_{iso} is higher in solvents with high ϵ than in solvents with low ϵ, the form of the ϵ dependence being a rapid rise as ϵ increases to about 10 and then levels off when $\epsilon \gg 1$. This solvent effect can be understood as a perturbation of the electronic structure of the N−O group. Polarity changes in the surrounding media induce shifts in the spin density; i.e., a more polar solvent causes an increased spin density on the nitrogen atom and thereby a stronger interaction between the free electron and the nitrogen nucleus, resulting in a higher A_{iso}. In protic solvents, A_{iso} is further increased ($A_{iso}^{h} > 0$). Thus, A_{iso} is higher in protic solvents than in aprotic solvents with similar ϵ; similar trends are expected for A_{zz}.[24]

The solvent dependence of the isotropic g-value (g_{iso}) shows a decrease in the g-value as a result of increased polarity of the solvent or hydrogen bonding with g_{xx} having the dominant effect. An increased solvent polarity shifts spin density from the oxygen to the nitrogen within the N−O bond (using the conventional molecular axes notation system with the x-axis along the N−O bond and the z-axis perpendicular to the nitroxide ring plane). The formation of hydrogen bonds affects the spin label g-tensor parameters via three separate effects: (1) transfer of spin density from the oxygen to the nitrogen atom, (2) increase of the $n\pi^*$ excitation energy, resulting in a lower g_{xx} value, and (3) transfer of some electron density from the lone-pair orbitals at the NO oxygen to the hydrogen donated in the hydrogen bond. This has been shown earlier in several studies employing various nitroxide spin labels in different environments.[25] An example of the use of polarity effects on A- and g-values is from the work of Steinhoff et al.[25] with bacteriorhodopsin (BR). The decrease in g_{xx} of ∼0.00035 reflects the change of ϵ from ∼25 to ∼80 in the vicinity of the aminoxyl, when moving through the BR proton channel from the cytoplasmic to the extracellular side. An increase in A_{zz} from 3.5 to 3.67 mT confirms these changes in dielectric constant in the protein. Similar results have been observed in membranes to determine polarity profiles.[26] Key to this[26] and in particular an earlier study[27] has been the use of spectral fitting, similar to that done in this paper. The spectral fitting enabled the demonstration of small, but significant changes in spectral parameters. Moreover, fitting algorithms provide estimates of parameter uncertainty, which allow estimates of parametric uncertainty based on variation of the spectral data from the fit hypothesis.

Further, temperature effects on ^{14}N hyperfine splittings have been noted by Bales et al.,[28] in which a typical increase of ∼14.5 μTesla is reported between 10 and 50 °C. Finally, aminoxyl concentration effects on the hyperfine splitting have been demonstrated.[21a,b]

The ultimate interpretation of the calculations must be tempered by their being performed in vacuo such that the exact nature of the conformational contributions cannot be unambiguously assigned. The consistency of these data with available experimental findings, including the ability to adequately model the experimental EPR spectrum, suggests that the results are indicative of the experimental observation. It is anticipated that similar combined theoretical and experimental investigations will be useful for atomic detail interpretation of EPR spectra. Such an approach, applied here, clarifies a nearly 30-year misconception that continues to pervade the spin-trapping literature.

(24) Owenius, R.; Engström, M.; Lindgren, M.; Huber, M. *J. Phys. Chem. A* **2001**, *105*, 10967−10977.
(25) Steinhoff, H. J.; Savitsky, A.; Wegener, C.; Pfeiffer, M.; Plato, M.; Möbius, K. *Biochim. Biophys. Acta* **2000**, *1457*, 253−262.
(26) Marsh, D. *Proc. Natl. Acad. Sci. U.S.A.* **2001**, *98*, 7777−7782.
(27) Bales, B. L.; Blum, R. A.; Mareno, D.; Peric, M.; Halpern, H. J. *J. Magn. Reson.* **1992**, *98*, 299−307.
(28) Bales, B. L.; Peric, M.; Lamy-Freund, M. T. *J. Magn. Reson.* **1998**, *132*, 279−286.

Experimental Section

Chemicals. All buffers were of reagent grade and were passed through a Chelex-100 ion exchange column to remove trace metal ion impurities prior to use. Superoxide dismutase, xanthine oxidase, hypoxanthine, diethylenetriaminepentaacetic acid (DTPA), and catalase were purchased from commercial sources. The spin traps 5,5-dimethyl-1-pyrroline *N*-oxide (DMPO) and 3,3,5,5-tetramethyl-1-pyrroline *N*-oxide (M_4PO) were synthesized as described in the literature,[29] purified by Kugelrohr distillation, and stored at −80 °C under N_2.

Superoxide Detection. Superoxide was generated by the action of xanthine oxidase, dialyzed against deferoxamine[30] (1 mM), on hypoxanthine (400 μM), DTPA (1 mM), and 50 mM sodium phosphate, pH 7.8. The rate of $O_2^{\bullet-}$ production was 10 μM/min at 25 °C. For experiments conducted in D_2O, the above reagents were dissolved in that solvent. Measurement of $O_2^{\bullet-}$ generation was estimated by monitoring the reduction of ferricytochrome *c* at 550 nm, in the absence and presence of SOD (30 U/mL), using an extinction coefficient of 20 mM^{-1} cm^{-1}.[31]

Spin-Trapping Superoxide and Hydroxyl Radicals. For spin-trapping $O_2^{\bullet-}$, experiments were conducted by mixing hypoxanthine (400 μM), DTPA (1 mM), and DMPO (100 mM) or M_4PO (100 mM) in 50 mM sodium phosphate, pH 7.8, in a final volume of 0.5 mL. The reaction was initiated by the addition of xanthine oxidase. Reaction mixtures were then transferred to a flat EPR quartz cell and fitted into the cavity of an E-9 EPR spectrometer. EPR spectra were recorded at 25 °C. For experiments conducted in D_2O, the above reagents (using only DMPO) were dissolved therein. For spin-trapping $HO^{\bullet}$, $FeSO_4$ (100 μM) was added to an aqueous solution of H_2O_2 (88 mM) and DMPO (100 mM) to a final volume of 0.5 mL. The reaction mixture was placed into a flat EPR quartz cell and fitted into the cavity of the spectrometer. EPR spectra were recorded at 25 °C. Spectrometer settings were the following: microwave power, 20 mW; modulation frequency, 100 kHz; modulation amplitude, 1.0 G; sweep time 12.5 G/min; response time 1 s. Receiver gains are presented in Figure 1.

Quantum-Mechanical Computations. Ab initio quantum mechanical studies were performed with the Gaussian94 package.[32] Calculations were performed at the unrestricted Hartree−Fock (UHF) level, using the 3-21G*, 6-31+G*, and 6-31++G** basis sets. Energy surfaces were obtained by constraining the specified dihedral and allowing all other degrees of freedom to relax. Puckering of the five-membered ring was defined based on the $C_2-C_3-C_4-C_5$ dihedral (Figure 2), with the transition state associated with flipping of the ring defined as $C_2-C_3-C_4-C_5 = 0.0$. Pucker 1 is defined as the ring pucker with the $C_2-C_3-C_4-C_5$ dihedral angle in the vicinity of 30° and pucker 2 as that with the $C_2-C_3-C_4-C_5$ dihedral angle in the vicinity of 30°. Fully optimized structures at the UHF/6-31++G** levels of theory were initiated from the minimum energy structures from the UHF/6-31+G* hydroxyl or hydroperoxide surfaces. Test calculations on the rotation of the hydroperoxyl hydrogen atom (e.g. for the C−O−O−H dihedral), at the UHF/3-21G* level, were performed on DMPO-OOH and M_4PO-OOH. Three energy surfaces were obtained, one with DMPO-OOH with the N−C−O−O dihedral constrained to 60° and two with M_4PO-OOH with the N−C−O−O dihedral constrained to 60° and 270°. In all cases a single mininum was obtained indicating that alternate minima associated with the orientation of the hydroperoxyl hydrogen atom are not complicating the N−C−O−O surfaces in Figures 4C,D and 5C,D.

Acknowledgment. This research was supported in part by grants from the National Institutes of Health, RR-12257, EB-2034, and GM-65944, and NIEHS and by the University of Maryland, School of Pharmacy, Computer-Aided Drug Design Center. We wish to thank Dr. Chris Felix of the National Biomedical EPR Center of the Medical College of Wisconsin in Milwaukee, WI for access to the S-band EPR spectrometer.

Supporting Information Available: Quantum mechanical data for Table 5 and Figure 6. This material is available free of charge via the Internet at http://pubs.acs.org.

JO0354894

(29) Bonnett, R.; Brown, R. F. C.; Clark, V. M.; Sutherland, I. O.; Todd, A. *J. Chem. Soc.* **1959**, 2094−2102.
(30) Gutteridge, J. M. C. *FEB Lett.* **1987**, *214*, 362−364.
(31) Kuthan, H.; Ullrich, V.; Estabrook, R. W. *Biochem. J.* **1982**, *203*, 551−558.
(32) Frisch, M. J.; Trucks, G. W.; Schlegel, H. B.; Gill, P. M. W.; Johnson, B. G.; Robb, M. A.; Cheeseman, J. R.; Raghavachari, K.; Al-Laham, M. A.; Zakrzewski, V. G.; Ortiz, J. V.; Foresman, J. B.; Cioslowski, J.; Stefanov, B. B.; Nanayakkara, A.; Challacombe, M.; Peng, C. Y.; Ayala, P. Y.; Chen, W.; Wong, M. W.; Andres, J. L.; Replogle, E. S.; Gomperts, R.; Martin, R. L.; Fox, D. J.; Binkley, J. S.; Defrees, D. J.; Baker, J.; Stewart, J. J. P.; Head-Gordon, M.; Gonzalez, C.; Pople, J. A. *Gaussian 94*, C.3 ed.; Gaussian, Inc.: Pittsburgh, PA, 1996.